International Organisation of Vine and Wine
Intergovernmental Organisation

Available on IVES Conference Series vine & wine

DOI : https://doi.org/10.58233/UvBMky9R

Characterization of winegrape berries' composition on sorting tables using hyperspectral imaging and AI

María P. Diago[1,2], Aitana Tejada[1,2], Ignacio Barrio[1,2], Wenchao Sheng[1], Juan Fernández-Novales[1,2], Leticia Martínez-Lapuente[1,2], Zenaida Guadalupe[1,2]

[1] Departamento de Agricultura y Alimentación. Universidad de La Rioja. Madre de Dios 53, 26006. Logroño. La Rioja (Spain).
[2] Instituto de Ciencias de la Vid y del Vino. Finca La Grajera. Ctra. de Burgos Km. 6. 26007. Logroño. La Rioja (Spain).

Abstract. Comprehensive evaluation of grape composition at winery receiving areas often requires multiple measurements to ensure representativeness, as well as the use of analytical techniques that are time-consuming and involve sample preparation. Recent advances in non-destructive sensing technologies, particularly hyperspectral imaging (HSI), offer promising alternatives for rapid and reliable grape quality assessment. In this context, the present study proposes a novel, non-invasive methodology for the characterization of winegrape composition directly on sorting tables. Specifically, hyperspectral imaging (HSI) in the visible to near-infrared range (400–1000 nm), combined with multivariate statistical analysis and artificial intelligence (AI), was applied to estimate key compositional parameters including total soluble solids (TSS), pH, chromatic characteristics, anthocyanins, malic acid, tartaric acid, and yeast assimilable nitrogen (YAN). The highest predictive performance was obtained for pH (R^2_{CV} = 0.90), with malic acid (R^2_{CV} = 0.76) and total soluble solids (TSS; R^2_{CV} = 0.64) also showing strong predictive capacity. For the remaining parameters, models achieved moderate R^2_{CV} values (0.30–0.50), sufficient to support binary classification between high and low levels. These findings highlight the potential of HSI as a powerful approach for grape quality assessment and decision-making in outdoor settings, such as grape sorting tables.

1. Introduction

Nowadays, assessment and sampling for maturity at the weightbridge of a winery are usually carried out using automated sampling devices (e.g. Maselli mechanical core sampler) or smaller manual devices. Although widely adopted, these methods require multiple measurements to ensure representativeness [1], often resulting in delays during unloading and prolonged exposure of grapes to suboptimal environmental conditions—factors that could adversely affect fruit integrity and overall wine quality.

Among the main compositional parameters, total soluble solids (TSS), yeast assimilable nitrogen (YAN), pH and concentrations of the main organic acids in the berry, such as tartaric and malic acid, as well as the anthocyanin and total phenol concentrations are usually analyzed using spectroscopy and wet chemistry procedures [2]. These analytical methods are destructive, time-consuming and require sample preparation in most instances. Therefore, it would be valuable for wineries to have rapid, robust and non-destructive methods to assess quality during grape receival.

Hyperspectral imaging (HSI) is a non-destructive technology in which a camera records the reflected light

from the target in specific regions of the electromagnetic spectrum in several tens or hundreds of narrow wavelengths. HSI integrates imaging and spectroscopy to obtain spatial and spectral data in one system [3]. The interaction between light at each wavelength and the different materials can be variable. When this interaction is measured, a unique individual 'fingerprint' called spectral signature is obtained. This holds distinctive quantifiable information that enables to reveal sample's hidden information by identifying "non-visible" features, such as chemical composition [3]. Its contactless and solvent-free nature, coupled with fast acquisition rates, makes it particularly suitable for real-time applications in both vineyard and winery environments. Nevertheless, challenges remain in terms of system cost and the

complexity of data analysis, although recent developments in AI and user-friendly software are significantly mitigating these constraints.

Hyperspectral imaging (HSI) has been extensively explored over the past decade as a powerful non-destructive technique for the inspection of food and unprocessed agricultural products [4, 5]. Its dual capability to perform both predictive analysis (via regression) and classification has rendered it particularly valuable in the agri-food sector, where it has been widely applied to assess fruit ripeness and composition [6,7]. In the case of grape berries, various studies have demonstrated the potential of contactless HSI in the visible and short-wave near infrared (Vis-SW NIR) range under laboratory conditions. For instance, Vis-SW NIR data —spanning from 380 to 1028 nm— acquired at a fixed distance from intact berries enabled to fingerprint the anthocyanin profile of eight different Vitis vinifera L. red cultivars [7]. In another study [8], contactless Vis-SW NIR (570-1000 nm) and NIR (1100-2100 nm) spectroscopy, performed at 25 cm from grape berries (under laboratory conditions) proved effective to estimate total soluble solids (TSS) (R2P ~0.90; SEP~1.60 ºBrix) and 22 free amino acids (with R2P varying from 0.30 to 0.66). Very recently, HSI data in the range from 400-1000 nm and NIR spectroscopy in the range 1200-2100 nm proved effective to estimate the volatile composition (up to 20 different volatile compounds were quantified) of Vitis vinifera L. Tempranillo Blanco berries during ripening under laboratory conditions [9, 10].

Although significant progress has been made, most of the research has been carried out under controlled laboratory conditions, where standardized distance to the target, consistent lighting, and stable environmental factors facilitate optimal hyperspectral image acquisition. To bridge this gap, recent research efforts have focused on adapting HSI technology for in-field and on-site applications. For example, a push-broom Vis-SW NIR HSI system mounted on a mobile platform was successfully employed in vineyards to acquire on-the-go measurements at approximately 5 km/h and 30 cm from the canopy, with spectral data correlated to laboratory analyses of cluster and berry samples of Tempranillo (Vitis vinifera L.) at different sampling dates from veraison to harvest during two seasons [11, 12].

Given that the receiving-crushing area of a winery can also be considered an outdoor scenario—characterized by variable temperature, humidity, lighting conditions, and inconsistent distances to the grape clusters—this study builds upon previous research by developing a modular structure to hold and operate an HSI system and additional set up, including artificial lighting and acquisition system, intended for its installation above sorting tables in commercial wineries. The aim of this work is to enable the in situ estimation of key compositional parameters of incoming grape loads. As such, HSI in the Vis-NIR (400-1000 nm) in combination with AI methods, has been used to build estimation models for a wide range of grape compounds in berries of grapevine Vitis vinifera L. Tempranillo. This approach may represent a significant step forward in both scientific and technological terms, as it broadens grape quality evaluation beyond conventional metrics of technological maturity, while also establishing the basis for the future non-invasive assessment of secondary metabolites such as phenolic and volatile compounds, highly related to wine quality but typically analyzed through time-consuming, expensive, and destructive laboratory procedures that require complex sample preparation and advanced instrumentation (e.g., HPLC/UPLC and GC-MS).

2. Materials and methods

The study was conducted in three main stages. The first stage involved hyperspectral imaging (HSI) data acquisition along with chemical analysis of the imaged grape samples. The second stage comprised the processing of hyperspectral images to automate the extraction of grape berry spectra, followed by the compilation of datasets. In the final stage, the dataset was used to train various predictive models using multivariate statistical analysis combined with artificial intelligence (AI).

2.1. Experimental layout

The *Vitis vinifera* L. Tempranillo clusters were collected during the 2024 season in a vineyard owned by La Rioja Government, located in Finca La Grajera (Logroño, La Rioja, Spain). The exact location of the vineyard plot is: 42º26’46.6’’ north latitude 2º30’41.6’’ west latitude; 450 m above sea level. The grapevines were grafted onto Ritcher 110 rootstock and were trained to a vertically shoot positioned system (VSP). The vineyard was planted in 2020 in an NW-SE orientation, and with a spacing between rows and within the row of 2.80 m × 1.20 m, respectively. The clusters were hand-picked randomly. Samples were collected from veraison to postharvest along seven dates: 12 August 2024, 19 August 2024, 24 August 2024, 2 September 2024, 9 September 2024, 16 September 2024 and 30 September 2024. For each date, the clusters were handpicked and immediately stored at -20ºC at the laboratories of the Institute of Sciences of Vine and Wine (ICVV, Rioja, Spain) until sample preparation.

2.2. Vis-SW NIR hyperspectral imaging

Prior to image acquisition, the clusters were allowed to thaw in a cold room (4ºC) and subsequently to ambient temperature (~20ºC). The clusters were dried prior to the acquisition with a kimwipe paper and were not further manipulated or destemmed.

Hyperspectral images were acquired at winery premises using a push broom Resonon Pika L VNIR hyperspectral imaging camera (Resonon, Bozeman, MA, USA) connected to an industrial computer. The spectral resolution of the camera was 2.1 nm (300 bands from 400 to 1000 nm), with 300 pixels of spatial resolution. External illumination has been provided with twelve 45W tungsten halogen lightbulbs. Prior to the hyperspectral measurement, a Spectralon® (Labsphere, Sutton, NH,

USA) white reference (a surface with a reflectance over 95%) was presented to the camera simulating the same position and distance to the fruit. A dark reference measurement was also performed to obtain the inherent electronic noise. The spectral light intensity values collected by the camera were translated into reflectance (R) with Equation 1:

$$R(\lambda) = \frac{G(\lambda) - D(\lambda)}{W(\lambda) - D(\lambda)} \quad (1)$$

where λ is a wavelength (in nanometers), G is the intensity of the light reflected by the grapes (in nanometers), W is the intensity of the light coming from the white reference (in nanometers), and D is the dark current (in nanometers).

To carry out the HSI acquisition, a holding structure was built and placed above the sorting table of the University of La Rioja (UR, Rioja, Spain) winery (Figure 1). In this structure, the HSI camera with the external illumination system were installed perpendicularly to the sorting table at 1 m distance.

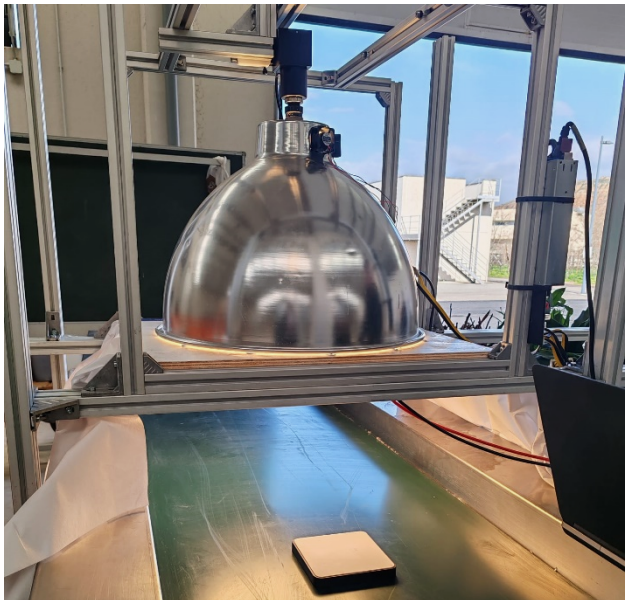

Figure 1. Hyperspectral imaging setup with Resonon Pika L VNIR camera and tungsten lighting above the sorting table, and Spectralon® white reference.

The hyperspectral images were acquired by placing the clusters on the sorting table, allowing at least 2 cm of separation between them to facilitate the later segmentation of the region of interest (ROI) corresponding to each one of the clusters.

For each one of the hyperspectral images acquired, a 10x10cm Spectralon® square was placed before the samples, to have an optimal reference for the exact environmental lighting in that moment. The number of grape clusters included in a single image ranged from five to eight, depending on the bunch size and the number of samples of a given date. The bunches were marked with a small tape in the peduncle alternating colors red, brown and white, to ensure the same order was preserved. This tape was removed from the spectra in later processing stages. For each group of bunches, two opposite sides were scanned in individual images, preserving the same order and conditions.

The camera settings were configured at 60fps (16.33 ms per frame from the theoretical 16.66 ms, accounting for the camera processing time) and 3 dB of gain at the sensor. These parameters were identical in each session, because the lighting conditions were controlled and the external influence was kept to a minimum by blocking direct light on both sides of the sorting table. The inevitable variations were compensated with the Spectralon®.

A total of 18 hyperspectral cubes were acquired for each side, for a total of 36, not accounting for black or other spectra acquisition for calibration. These images contained a total of 97 individual clusters.

2.3. Analysis of grape composition

Once imaged, the clusters were destemmed and berries crushed manually. Thereafter, the samples were centrifuged (Sorvall Lynx 4000 Centrifuge, Thermo Scientific, Madrid, Spain).

Total soluble solids (TSS) and pH were measured using conventional OIV methods [13]. TSS was determined with a temperature compensating Quick-Brix 60 digital refractometer (Mettler Toledo, Columbus, OH, USA) adding a few drops of the centrifuged must, and expressed as °Brix. pH was measured with a PH 8 PRO benchtop pH meter (XS Instruments, Codogno, LO, Italy).

Malic acid, tartaric acid, anthocyanins and YAN amounts were determined using an enzymatic multiparameter analyser BioSystems Y-200 (BioSystems, Barcelona, Spain).

The chromatic characterization of the samples, including color intensity (CI), Total Polyphenol Index (TPI) —I_{280}—and colorimetric parameters (L, a, and b*), was carried out using an Agilent Cary 60 UV-Vis spectrophotometer (Agilent Technologies, Santa Clara, CA, USA).

2.4. Spectral data analysis

The HSI data were processed using Python 3.12 alongside widely adopted computer vision and machine learning libraries, including OpenCV [14], scikit-image and scikit-learn.

To automate the extraction of spectral signatures for each sample in the images, a representative subset of images was decomposed into all the individual wavelength bands and then saved as greyscale images. This allowed the identification of the optimal spectral range for distinguishing between the pixels belonging to the sorting table and the pixels belonging to the berries conforming the clusters. The most effective wavelengths in our setup ranged from 860 to 920 nm, with the optimal band varying slightly across acquisition sessions.

Otsu's thresholding method [15], combined with basic morphological operations to remove noise and small

regions, was employed to isolate the region of interest (ROI) corresponding to each individual sample cluster.

The resulting binary masks were then saved in combination with the RGB components (chosen at 640 nm, 550 nm and 460 nm respectively) of the hyperspectral image, then manually reviewed and corrected when necessary. Histogram equalization was applied to each band individually to improve the contrast of the images to review. Average spectra were subsequently calculated based on the pixels within the ROIs. A side-by-side comparison illustrating the resulting rectangular ROIs after segmentation is provided in Figure 2.

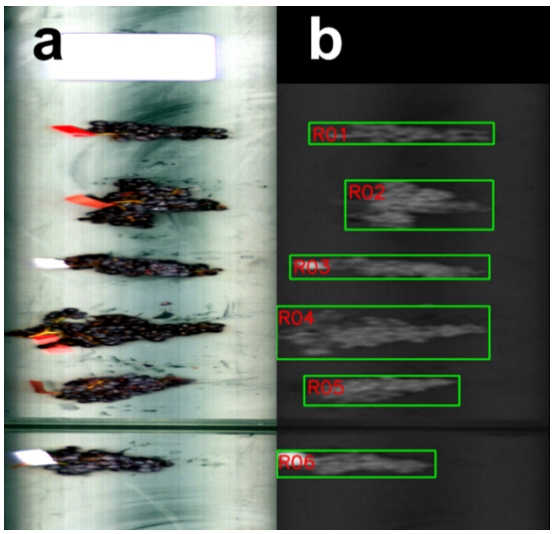

Figure 2. a) Contrast corrected RGB portion of a hyperspectral image and b) Rectangular regions covering each one of the ROIs.

Regression models using partial least squares (PLS), machine learning and artificial intelligence (ML/AI) algorithms have been built from the HSI data for all grape components, using cross validation as the main criteria, and performance metrics (R^2, RMSE) computed and compared. Due to the noisy nature of spectral data, a sizable amount of preprocessing becomes necessary in both classic and IA based methods [16]. Several preprocessing methods were evaluated in this study to enhance spectral data quality and modeling performance. These included the Savitzky–Golay filter [17] with a first-degree derivative and a window size of 15 for TSS, 19 for pH and for 17 tartaric acid. This filtering technique effectively reduced the intensity component of noise. Additionally, Mean Centering, Standard Normal Variate (SNV), and Autoscaling were applied to normalize the data and minimize variability unrelated to the chemical composition of the samples.

For the machine learning models, a hyperparameter optimization strategy based on a nature-inspired algorithm was employed in order to improve model performance while maintaining computational efficiency. Specifically, we used the Bat Algorithm (BA), which is inspired by the echolocation behavior of microbats, which use frequency tuning and loudness adaptation to efficiently explore their environment and converge toward optimal solutions [18].

The optimization procedure was configured to run for a maximum of 50 generations (epochs), with each generation comprising a population of 10 candidate solutions. An early stopping criterion based on performance stagnation was employed, terminating the search if no improvement was observed over 5 consecutive generations. This strategy effectively balances exploration and exploitation within the hyperparameter space. The algorithm was applied to tune only the most influential hyperparameters for each model, thereby minimizing the risk of overfitting and enhancing generalization capabilities. Model performance during optimization was assessed using 10-fold cross-validation, with the mean squared error (MSE) serving as the scoring metric. This approach ensures that the selected models exhibit consistent performance across different data subsets, not just the training data.

Overall, this nature-inspired optimization strategy provided an effective way to approach near-optimal solutions with fewer evaluations than exhaustive grid search methods, enabling faster development with limited computational resources.

3. Results and discussion

3.1. Grape composition

The parameters studied were well represented with an adequate variability; samples being taken from veraison to postharvest (Figure 2). Likewise, TSS varied between 10.8 °Brix to 27.0 °Brix, while pH ranged from 3.16 to 4.58. Tartaric acid concentrations spanned from 0.84 to 4.37 g/L, and malic acid from 1.73 to 8.58 g/L. Anthocyanin content showed a wide range, from 23 to 265 mg/L. Yeast assimilable nitrogen (YAN) levels varied markedly, between 35 and 512 mg/L. Chromatic parameters also exhibited notable variability: total polyphenol index (TPI) ranged from 8.27 to 37.78 UA, and color intensity (CI) from 1.40 to 7.42 UA. In terms of CIELAB coordinates, L* values ranged from 74.73 to 93.49, a* from 2.46 to 17.88, and b* from 1.04 to 13.29, capturing the evolution of grape skin color attributes over time.

3.2. Regression models for grape composition prediction

A baseline model was generated for each of the parameters using PLS technique, widely used in hyperspectral data processing due to the inherent reduction in dimensionality. While PLS regression remains a standard technique for handling collinear spectral data and performing dimensionality reduction [19], Random Forest Regressor (RF), Multilayer Perceptron Regressor (MLP), and other artificial intelligence driven approaches offer several notable advantages. These include an enhanced capability to model complex nonlinear relationships between spectral variables and grape compositional traits, increased robustness to noise and irrelevant variables due to intrinsic feature selection and ensemble averaging, and

the ability to process high-dimensional spectral datasets without requiring stringent prior dimensionality reduction [20, 21].

Table 1 shows the models that provided the best results for cross-validation (CV), $R^2_{CV} > 0.4$, for Total Soluble Solids (TSS), pH, tartaric and malic acid. R^2 values between 0.30 and 0.50 are considered to provide good separation between high and low values. R^2 values between 0.50 and 0.70 provide good separation between high, medium, and low values. R^2 values between 0.70 and 0.90 are considered a good adjustment, and, finally, R^2 values ≥0.90 provide an excellent adjustment [9].

When RF and MLP models failed to achieve adequate predictive performance, PLS regression was employed as an alternative modeling approach to improve prediction accuracy. Among these, the best results were obtained for pH, with a RF model achieving a cross-validation coefficient of determination (R^2_{CV}) of 0.90 and a RMSECV of 0.11, indicating an excellent, predictive accuracy. A less robust outcome was observed for total soluble solids (TSS), where a MLP model reached an R^2_{CV} of 0.64 and $RMSE_{CV}$ of 2.40, indicating a good separation between high, medium, and low values. For malic acid, the PLS model performed slightly better, with an R^2_{CV} of 0.76 and $RMSE_{CV}$ of 0.59, which corresponds to a good level of model adjustment. In contrast, tartaric acid and the total polyphenol index (I_{280}) yielded more modest predictive capacity, with R^2 values of 0.41 and 0.42, respectively, still offering meaningful discrimination between high and low concentration ranges, though not suitable for precise quantification.

Table 1. Cross-validation of the best models obtained to predict the grape composition parameters from HSI.

Parameters	Model	$RMSE_{CV}$	R^2_{CV}
Total soluble solids (º Brix)	MLP	2.40	0.64
pH	RF	0.11	0.90
Tartaric acid (g/L tartaric acid)	RF	0.63	0.41
Malic acid (g/L malic acid)	PLS	0.59	0.76
Total Polyphenol Index (I_{280})	PLS	4.24	0.42

MLP: Multi Layer Perceptron. RF: Random Forest. PLS: Partial Least Squares. R^2_{CV}: determination coefficient of calibration. $RMSE_{CV}$: root mean square error of cross validation.

Several other grape composition parameters exhibited limited predictive performance, with coefficient of determination (R^2_{CV}) values falling below 0.40. These include yeast assimilable nitrogen (YAN), with an R^2_{CV} of 0.35 and an $RMSE_{CV}$ of 75, and the color intensity (CI), for which the model achieved an R^2_{CV} of 0.30 and an $RMSE_{CV}$ of 0.97. Similarly, total anthocyanin concentration (R^2_{CV} = 0.31; $RMSE_{CV}$ = 44), as well as the CIELab color coordinates L* (R^2_{CV} = 0.30; $RMSE_{CV}$ = 3.03), a* (R^2_{CV} = 0.31; $RMSE_{CV}$ = 3.13) and b* (R^2_{CV} = 0.62; RMSECV = 1.38), showed lesser predictive capacity, despite the comparatively higher R^2_{CV} value of the b*. These results fall within the category of models that provide only a basic separation between high and low values ($0.30 \leq R^2_{CV} < 0.50$). Notably, all models for these parameters were developed using PLS regression, as the implementation of machine learning algorithms did not result in improved predictive accuracy.

Figure 3 displays the best prediction models for grape parameters showing adequate prediction capacity from hyperspectral imaging. The samples gathered in the regression plots for pH (Figure 3a), total soluble solids (Figure 3b) and malic acid (Figure 3c) show a really good fit along the correlation lines and mostly fitted between the 95% confidence bands. A considerably large and evenly distributed range for the studied parameters was covered by the samples from the experiment.

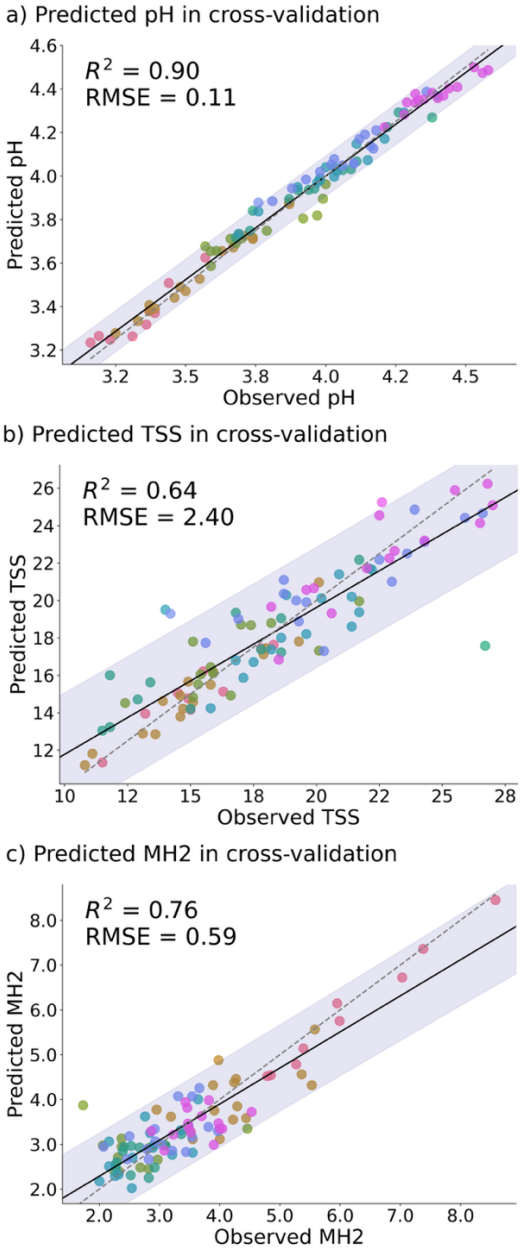

Figure 3. Regression plots for pH (a), Total Soluble Solids (b) and Malic acid (c) using the best models generated from grape clusters hyperspectral images in the VIS + SW-NIR range. Solid line represents the regression line and dotted line refers to the 1:1 line. Prediction confidence bands are shown at a 95% level (semitransparent area). Different dot colors correspond to different sampling dates (lower hue indicates earlier dates).

The tendency exhibited in Figure 3 is consistent with expected physiological trends during grape ripening, where malic acid degradation is accompanied by rising pH levels and an increase in total soluble solids due to sugar accumulation.

The results of this work are consistent with, albeit slightly below, the state-of-the-art in hyperspectral imaging (HSI) applications for grape quality prediction under laboratory or field conditions [9, 11, 12].

Better predictive performance for total soluble solids (TSS) has been consistently demonstrated in previous research, with R^2CV values nearing 0.90 [9, 11, 12]. In contrast, the model developed in the present study yielded a lower R^2_{CV} of 0.64, which still permits effective stratification of grape samples into three categories (low, medium, and high °Brix). Such categorical discrimination remains highly valuable for practical applications at grape reception in the winery, facilitating informed decisions regarding batch classification and optimal vinification strategies.

PLS regression models reported in [12] achieved higher R^2_{CV} values of 0.84 for malic acid and 0.56 for tartaric acid compared to those obtained in the present study (0.76 and 0.41, respectively). However, their informed $RMSE_{CV}$ values were 0.90 g/L for malic acid and 1.29 g/L for tartaric acid, while the present study achieved lower $RMSE_{CV}$ values, 0.59 g/L and 0.63 g/L, respectively, indicating improved predictive accuracy in absolute error terms despite lower coefficient of determination values.

Noteworthy, the predictive performance achieved for pH in this study (R^2_{CV} = 0.90; $RMSE_{CV}$ = 0.11) stands out. This result not only falls within the category of models with an excellent fit but also surpasses previously reported values in the literature (R^2_{CV} = 0.73; $RMSE_{CV}$ = 0.20) using PLS regression under field conditions with VIS-NIR hyperspectral imaging [12].

Concerning chromatic parameters, prior literature have reported superior predictive performance for anthocyanin concentration, with R^2_{CV} values of 0.83 using support vector machines (SVM) and 0.78 using PLS regression models based on on-the-go hyperspectral imaging in commercial vineyards [11,12]. Similarly, for the total polyphenol index, an R^2_{CV} value of 0.44 was reported by the same authors, which is comparable to the results obtained in the present study.

However, several methodological and experimental differences must be considered when interpreting these outcomes. Contrary to prior studies that conducted hyperspectral imaging on freshly harvested or field-collected grape clusters [7, 11, 12], the hyperspectral data in this study were acquired following the freezing and subsequent thawing of the grape samples. This protocol, implemented due to logistical and experimental constraints, may have compromised tissue integrity, thereby influencing the reflectance properties, particularly within wavelength regions sensitive to water content, pigment distribution, and surface structure. Such alterations in spectral responses could partially explain the diminished data quality, potentially limiting the accuracy of predictive models derived from these images.

Another notable divergence from literature is the choice of modeling approach. While most previous studies employed PLS regression [7, 9, 12], the present research explores the potential of RF algorithms and MLP, non-parametric machine learning methods with several advantages in the context of high-dimensional spectral data [22, 23]. Unlike PLS, which primarily captures linear relationships, RF and MLP are capable of modeling complex, non-linear interactions and can automatically identify and prioritize relevant spectral features, offering improved generalization when appropriately trained. Moreover, RF and MLP tend to be more robust to multicollinearity, outliers, and non-Gaussian data distributions, making it a valuable tool in scenarios where spectral variability is high or dataset quality is heterogeneous [24].

Despite the relatively modest performance observed for certain chemical parameters, the use of RF, MLP and similar artificial intelligence techniques represents a strategic advancement in the application of HSI to viticulture. As datasets grow in volume and diversity, and as more sophisticated preprocessing and model-tuning techniques are implemented, machine learning models are expected to surpass traditional linear approaches in both accuracy and adaptability—particularly for agricultural applications [24, 25].

4. Conclusions

This preliminary study demonstrates the feasibility of applying HSI combined with AI techniques to assess grape composition with a non-destructive, rapid, and scalable approach. Among the regression models developed, pH prediction achieved the highest performance (R^2_{CV} = 0.90), considered to provide an excellent adjustment. Notably, the models developed for total soluble solids (TSS) and malic acid achieved sufficient predictive power (R^2_{CV} = 0.64 and 0.76, respectively) to enable the reliable classification of grape samples into three categories—low, medium, and high values—thus offering valuable decision-making support at grape reception. For other compositional traits, including tartaric acid, yeast assimilable nitrogen, total polyphenol index, anthocyanins, color intensity and chromatic coordinates, the models yielded R^2_{CV} values between 0.30 and 0.50. While these results do not allow for precise quantitative predictions, they are nonetheless adequate to distinguish between high and low concentration levels, providing a useful basis for initial sorting and qualitative assessment.

Despite the relatively modest performance observed for some chemical traits compared to other studies, the use of AI techniques like Random Forest (RF) and Multilayer Perceptron Regressor (MLP) represents a strategic advancement in viticultural applications of HSI. As datasets grow in volume and diversity, and as more sophisticated preprocessing and model-tuning techniques are implemented, machine learning models are expected to

outperform classical chemometric methods in both accuracy and adaptability—particularly for in-field, real-time monitoring scenarios.

It is worth highlighting that this study is framed within the HyperGrape project (PID2023-150555OB-I00, funded by MCIU/AEI/10.13039/501100011033 and by FEDER, EU), which aims to overcome current limitations in the assessment of grape composition and quality. Beyond the parameters analyzed in the present work, the project's overarching objective is to develop robust, real-time, and non-invasive methodologies for monitoring the evolution of key phenolic (e.g. anthocyanins, flavonols, flavanols, hydroxycinnamic acids, and stilbenes) and volatile (e.g. terpenes, norisoprenoids, C_6 compounds, and benzenoids) compounds, in red and white grape cultivars, both in winery and vineyard settings. In forthcoming studies, a dual-camera system incorporating the Pika IR+ sensor will be implemented, extending spectral coverage (400–1700 nm). This broader spectral window is expected to enhance the system's ability to capture complex chemical signatures, thereby enhancing the accuracy and adaptability of predictive models.

In conclusion, the integration of HSI sensors within the crush pad environment, in combination with advanced AI-driven modelling, holds the potential to generate rapid, objective, and non-invasive predictions of grape quality and composition. This, in turn, may enhance winemaking practices by improving both perceived quality and compliance with quality assurance standards. In the longer term, the implementation of such technologies could support the development of more transparent and data-driven grape purchasing frameworks, reflecting the true compositional value of the fruit and informed by the input of key stakeholders across the wine value chain.

5. References

1. W. Allan, *Winegrape Assessment in the Vineyard and at the Winery* (Grape and Wine Research and Development Corporation, Adelaide, 2003)
2. R. B. Boulton, V. L. Singleton, L. F. Bisson, R. E. Kunkee, *Principles and Practices of Winemaking* (Chapman & Hall, New York, 1996)
3. H. Grahn, P. Geladi, *Techniques and Applications of Hyperspectral Image Analysis* (John Wiley & Sons Ltd, Chichester, 2007)
4. D. Wu, D. W. Sun, Innov. Food Sci. Emerg. Technol. **19**, 1–14 (2013)
5. M. Sun, D. Zhang, L. Liu, Z. Wang, Food Chem. **218**, 413–421 (2017)
6. B. Li, M. Cobo-Medina, J. Lecourt, N. Harrison, R. J. Harrison, J. V. Cross, Postharvest Biol. Technol. **141**, 8–15 (2018)
7. M.P. Diago, J. Fernández-Novales, A. M. Fernandes, P. Melo-Pinto, J. Tardáguila, J. Agric. Food Chem. **64**, 7658–7666 (2016)
8. J. Fernández-Novales, T. Garde-Cerdán, J. Tardáguila, G. Gutiérrez-Gamboa, E. P. Pérez-Álvarez, M. P. Diago, Talanta **199**, 244-253 (2019)
9. S. Marín-San Román, J. Fernández-Novales, C. Cebrián-Tarancón, R. Sánchez-Gómez, M. P. Diago, T. Garde-Cerdán, J. Agric. Food Chem. **71**, 2616-2627 (2023)
10. S. Marín-San Román, J. Fernández-Novales, C. Cebrián-Tarancón, R. Sánchez-Gómez, M. P. Diago, T. Garde-Cerdán, J. Sci. Food Agric. **103**, 6317-6329 (2023)
11. S. Gutiérrez, J. Tardáguila, J. Fernández-Novales, M. P. Diago, Aust. J. Grape Wine Res. **25**, 127-133 (2019)
12. J. Fernández-Novales, I. Barrio, M. P. Diago, Agronomy **11**, 2534 (2021)
13. OIV, *Compendium of International Methods of Wine and Must Analysis* (International Organisation of Vine and Wine, Dijon, 2024)
14. G. Bradski, Dr. Dobb's J. Softw. Tools **25**, 120–125 (2000)
15. N. Otsu, IEEE Trans. Syst. Man Cybern. **9**, 62–66 (1979)
16. M. Vidal, J. M. Amigo, Chemom. Intell. Lab. Syst. **117**, 138–148 (2012)
17. A. Savitzky, M. J. E. Golay, Anal. Chem. **36**, 1627–1639 (1964)
18. X. S. Yang, X. He, Int. J. Bio-Inspir. Comput. **5**, 141–149 (2013)
19. S. Wold, M. Sjöström, L. Eriksson, Chemom. Intell. Lab. Syst. **58**, 109–130 (2001)
20. B. Lu, Y. He, P. D. Dao, IEEE J. Sel. Top. Appl. Earth Obs. Remote Sens. **12**, 1784–1797 (2019)
21. G. E. Hinton, Artif. Intell. **40**, 185–234 (1989)
22. L. Breiman, Mach. Learn. **45**, 5–32 (2001)
23. F. Murtagh, Neurocomputing **2**, 183–197 (1991)
24. Y. E. García-Vera, A. Polochè-Arango, C. A. Mendivelso-Fajardo, F. J. Gutiérrez-Bernal, Sustainability **16**, 6064 (2024)
25. Khan, A. D. Vibhute, S. Mali, C. H. Patil, Ecol. Inform. **69**, 101678 (2022